PCCP

Accepted Manuscript

ROYAL SOCIETY OF CHEMISTRY

www.rsc.org/pccp

Theoretical Study on Dehydrogenation Reaction of Dihydrogen Bonded Phenol-Borane-Trimethylamine in Excited State

Yonggang Yang,[a] Yufang Liu, *[a] Dapeng Yang,[b] Hui Li,[a] Kai Jiang,[c] Jinfeng Sun[a]

[a] *College of Physics and Information Engineering, Henan Normal University, Xinxiang 453007, China.*

[b] *Physics Laboratory, North China University of Water Resources and Electric Power, Zhengzhou 450045, China*

[c] *College of Chemistry and Environmental Science, Henan Normal University, Xinxiang 453007, China*

* Corresponding Author. Tel: +86-373-3329297; Fax: +86-373-3329297.
E-mail: yf-liu@henannu.edu.cn (Y.F. Liu).

Abstract:

Time dependent density functional theory (TDDFT) and transition state theory (TST) have been performed to study the dehydrogenation process of dihydrogen bonded phenol-borane-trimethylamine (phenol-BTMA) in excited state. The potential curve of phenol-BTMA in the ground state confirms that the dehydrogenation process does not occur in the ground state. The analysis of geometric structure and infrared spectra demonstrates that dihdyrogen bond O-H•••H_1-B of phenol-BTMA is considerably strengthened with the cleavage of O-H when being excited to the first excited state. Based on the geometric structure in the first excited state, a transition state is found with the only imaginary frequency pointing to the formation of hydrogen molecule. This finding implies the occurrence of dehydrogenation process of phenol-BTMA in excited state. Dehydrogenation reaction is fully completed in the reaction product and the new formed hydrogen molecule moves away from the plane of benzene ring. This work provides a theoretical model for the dehydrogenation process of phenol-BTMA in the excited state.

1. Introduction

As a ubiquitous phenomenon in many branches of science, hydrogen bonds is central to understanding the microscopic structure and the function in many molecular systems, such as proteins and DNA building blocks of the life.[1-8] In recent years, excited state hydrogen bond dynamics is widely used to interpret the photochemical and photophysical properties and the dynamic behaviors of hydrogen bonded molecular.[9-17] As an unconventional hydrogen bond, dihydrogen bond is the interaction between oppositely charged hydrogen atoms and can be represented as D-H(δ+)•••(δ-)H-A, wherein D and A are respectively electronegative and electropositive elements with respect to hydrogen.[18-26] When the intermolcular dihydrogen bond interaction becomes so strong that B-H and D-H bonds are both cleaved, the two hydrogen atoms with opposite charges attract each other and the dehydrogenation reaction will occur.

As a perfect green energy, hydrogen has much larger energy than that of the fossil fuels. Even more importantly, the combustion product of hydrogen is water, while that of fossil fuels are noxious gas which are undesirable to the human body and the environment. [27] Dihydrogen bond has been confirmed as a key intermediate in the dehydrogenation process of metal hydrides.[28-32] The study of dihydrogen bond and its dehydrogenation reaction have drawn greater attention in recent years.[28-32] Apart from metal hydrides, borane-amines is a promising material due to its high hydrogen content and the fact that a variety of transition metal compounds, have the ability of promoting its kinetically controlled dehydrogenation.[27,33] Therefore, the

dehydrogenation reactions of borane-amines molecular along dihydrogen bond have attracted much attention.

Laser induced fluorescence (LIF) excitation and fluorescence detected infrared (FDIR) are adopted to study the complex between borane-dimethylamine (BDMA) and phenol, in order to confirm the formation of dihydrogen bond.[34] The formation of dihydrogen bond has been demonstrated by studying the non-covalent intermolecular interaction between borane-trimethylamine and acetylene, fluoroacetylene, and other solvents.[34-35] The dihydrogen bonds between boron-amine and acidic hydrogen donors, such as phenol, aniline, 2-pyridone, have been reported in the gas phase.[36-41] Proton transfer is found to be an important step in many chemical and biological reactions.[42-43] Therefore, the studies of boron hydrides reactivity have focused on their role in such reactions with proton transfer and H_2 evolution.[31] The proton affinities of borane-amines have been demonstrated to be related to the elimination of H_2.[32] The intermolecular dihydrogen bond in $[(C_6F_5)_2(C_6Cl_5)B]$-H•••H-[TMP] has been reported for the study of the product of H_2 cleavage by an intermolecular frustrated Lewis pair (FLP).[44]

The dehydrogenation reaction of dihydrogen bonded phenol-BTMA in the gas phase has been reported by Patwari *et al*.[39] However, few theoretical perspectives on the properties of dihydrogen-bonded complexes in their electronic excited states have been reported so far, especially the dehydrogenation reaction upon photoexcitation.[45-46] In our previous work, we have desmonstrated that the N-H•••O hydrogen bond in the cyclic structure of phenol-BDMA complex hindered the

dehydrogenation reaction between dihydrogen bonded O-H and B-H_1 groups in excited state.[47] Transition state theory (TST) has been used widely to find out that how chemical reactions take place.[48-52] In this work, we will study the dihydrogen bond interaction of phenol-BTMA in order to study dehydrogenation process in excited state by using transition state theory.

2. Computational Methods

The geometric structure, electronic and infrared spectra, and potential curves of phenol-BTMA are calculated using Gaussian 09 program suite.[53] Becke's three-parameter hybrid exchange function with Lee-Yang-Parr gradient-corrected correlation functional (B3-LYP functional), in combination with 6-311++G(d, p) basis set, is used in the Density functional theoretical (DFT) [54-55]. The entire local minimums are confirmed by the absence of any imaginary frequency in vibrational analysis calculations. The CIS/ 6-311++G(d, p) method is used to search the transition state and product in the excited S_1 state. Based on the optimized geometry of phenol-BTMA in the S_1 state, potential energy curves scan is performed in order to find the Transition State and Product. The saddle point and minimum energy point of potential energy curves in the S_1 state were used as the starting point for the transition state calculation [using the command OPT=(TS, CalcFC)] and product calculation. One imaginary frequency was found, whose corresponding vibrational mode points to the formation of hydrogen molecule.

3. Results and Discussion

3.1 Optimized Geometric Structures in the Ground State and the S_1 State

The bond lengths and angles of the reactant complex (RC), transition state (TS) and product (P) in the ground state (S_0) and the first excited state (S_1) are denoted in Figure 1. The TS in the ground state is termed as TS-S_{00} in which the first zero denotes RC-S_0 and the second zero denotes ground state calculation. The transition states based on the RC-S_1 are denoted as TS-S_{10} and TS-S_{11} respectively for ground and the excited S_1 states calculation.

For RC-S_0, the calculated bond lengths of phenol-BTMA are in agreement with reference 39. The bond lengths of O-H and B-H_1, which are involved in the formation of O-H•••H_1-B, respectively lengthen about 0.052 Å and 0.024 Å. The bond lengths of dihydrogen bonds O-H•••H_1-B and O-H•••H_2-B are calculated respectively to be 1.870 Å and 2.252 Å in the ground state, which decrease to 1.387 Å and 2.117 Å when excited to the S_1 state. The two dihydrogen bonds of phenol-BTMA are both strengthened in the excited S_1 state, and the change of O-H•••H_1-B (0.483 Å) is significantly larger than that of O-H•••H_2-B (0.125 Å). This change indicates that the dehydrogenation reaction may occur along dihydrogen bond O-H•••H_1-B while not O-H•••H_2-B. The angles COH and OHH_1 are calculated to be 110º and 151º in the ground state and change to 115 º and 163 º when excited to the S_1 state, implying that the dihydrogen bond interaction of O-H•••H_1-B is prior to than that of O-H•••H_2-B.

In the TS-S_{10}, the bond length of O-H increases to 1.713 Å, indicating that the O-H bond is cleaved for the formation of H-H_1 bond. The angles COH and OHH_1 are calculated to be 110º and 165º in the ground state and change to 56 º and 143 º in the product, indicating that the geometric structure of P-S_{10} changes a lot compared with

that of TS-S_{10} and that the new formed hydrogen molecule moves away from phenol molecule. The bond length of intermediate product O-H•••H_1 is calculated to be 0.786 Å, which is considerably smaller than that of phenol-BTMA in RC-S_1 (1.387 Å). This difference indicates that the dihydrogen bond interaction O-H and B-H_1 is significantly strengthened in the TS-S_{10}, which induces the occurrence of dehydrogenation reaction. In the P-S_{10}, it is observed that the bond length of H-H_1 is 0.744 Å, which confirms the formation of hydrogen molecule. The newly formed hydrogen molecule moves away from the plane of benzene ring. Dehydrogenation process of phenol-BTMA occurs in P-S_{10} with the formation of molecule hydrogen. In the TS-S_{11}, the bond length of intermediate product O-H•••H_1 is calculated to be 0.751 Å, which is smaller than that of TS-S_{10} (0.786 Å) and lengthened to 0.777 Å in the P-S_1 state.

3.2 Potential Energy Curves

Figure 2 shows the potential energy curves of phenol-BTMA scanned on the bond length of O-H•••H_1-B in the S_0 and S_1 states. In Figure 2A, the energies of phenol-BTMA increase with the scanning of the bond length of O-H•••H_1-B from 1.9 Å to 0.5 Å. There is no obviously formed intermolecular dihydrogen bond between phenol and BTMA at the 1st point (from right to left). An intermolecular dihydrogen bond is formed at the 6th point, and a new intermediate B-H_1-O-H is formed in the 11th point. When locating at 13th point, the O-H bond is cleaved without new formed hydrogen molecule. That is, no dehydrogenation reaction occurs with the bond length of H•••H_1 being smaller than that of normal hydrogen molecule. In Figure 2B, an

intermolecular dihydrogen bond is formed in the 1st point (scanning from 1.39 Å to 0.69 Å). The energy of phenol-BTMA increases with the shortening of the bond length to the maximum point (the 6th point) which can be used in Transition State finding. After crossing the maximum point, the energy of phenol-BTMA decreases a lot. The energy located at 8th point is lower than that of the 1st point, which is used to find the product by using Transition Station Theory. It can be concluded that the dehydrogenation reaction of phenol-BTMA is based on the geometric structure in the S_1 state.

3.3 Energy Profile Analysis

Figure 3 shows the energy profile of phenol-BTMA in the ground and the excited S_1 state. In Figure 3A, the energies of phenol-BTMA in the ground and the S_1 states are set as zero so that the differences can be obtain directly. In the excited S_1 state, the energy of phenol-BTMA is calculated to be 97.47 kcal/mol, which is significantly larger than that in TS-S_{10} state (57.35 kcal/mol). Therefore, the dehydrogenation reaction of phenol-BTMA overcomes the energy barrier when being excited to the S_1 state. In the P-S_{10} state, the energy of phenol-BTMA decreases to -11.21 kcal/mol, which is slightly smaller than that of RC-S_0 in the ground state. In Figure 3b, the energy of TS-S_1 is calculated to be 18.87 kcal/mol and is lower than that of P-S_1, which does not meet the standard of Transition State Theory. It can be concluded that the dehydrogenation reaction of phenol-BTMA, based on the geometric structure in the S_1 state, occurs in the ground state while not the excited S_1 state. Figure 3 describes the dehydrogenation process of phenol-BTMA based on the geometric

structure in the S_1 state by using transition state theory.

3.4 Infrared Spectra Analysis

The infrared spectra of dihydrogen bonded phenol-BTMA in different states are provided in Figure 4 in order to delineate its dehydrogenation reaction clearly. Figures 4a and 4b denote the infrared spectra of RC in the ground sate and the excited S_1 state, and Figures 4c and 4d denote respectively those of TS-S_{10} and P-S_{10}. In Figure 4a, the stretching vibration peak of B-H_1 is calculated to be 2335 cm^{-1}, which is slightly smaller than the experimental result (2349 cm^{-1}), and those of B-H_2 and B-H_3 are consistent with experimental results. The stretching vibration peak of O-H bond is 3553 cm^{-1}, larger than that of experimental data (3514 cm^{-1}). When excited to the S_1 state, the functional groups involved in the formation of intermolecular hydrogen bond of phenol-BTMA are all red-shifted. The red-shifting of B-H_1 (164cm^{-1}) is significantly larger than those of B-H_2 (27 cm^{-1}) and B-H_3 (24cm^{-1}). The function group O-H red-shifts about 980 cm^{-1} (from 3553 cm^{-1} to 2673 cm^{-1}), which implies the formation of intermediate product (O-H•••H_1). In Figure 4c, it is obvious that the stretching vibration peak corresponding to B-H_1 disappears and that a new peak appears at 3528 cm^{-1} which corresponds to O•••H-H_1. These changes of infrared peaks indicate that the O-H bond is cleaved with a new bond H-H_1 formed, and that the newly formed H-H_1 is affected by the interaction between O and H atoms. Moreover, the only imaginary frequency located at -745.46 cm^{-1} appears in the infrared spectra results, which points into the formation of hydrogen molecule. In Figure 4d, it is noted that a new peak appearing at 4263 cm^{-1} corresponds to the stretching vibration

peak of H-H_1, which confirms the hydrogen elimination. The infrared spectra in Figure 4 demonstrate the dehydrogenation reaction of phenol-BTMA in the excited state indirectly.

3.5 Frontier Molecular Orbit Analysis

The analysis of molecular orbitals (MOs) can provide insight into the nature of the excited states and play a crucial role in the chemical stability of molecules.[56-57] The frontier molecular orbitals (MOs) of RC-S_1, TS-S_{10} and P-S_{10}, whose S_1 states are all corresponding to the highest occupied molecular orbital (HOMO)→the lowest unoccupied molecular orbital (LUMO) transition, are shown in Figure 5. For RC-S_1, it is noted that the electron densities of the HOMO are strictly localized on the phenol molecule, which indicates that only the phenol moiety has been electronically excited in the S_1 state. When excited to LUMO, the electron densities of phenol-BTMA transfer from phenol moiety to BTMA moiety. This transfer indicates that phenol-BTMA undergoes an intermolecular charge transfer process. The electron densities of O atom decrease when excited to the S_1 state, implying that the charge of H atom becomes more positive and that the dihydrogen bond interaction between O-H and B-H_1 is strengthened. In the TS-S_{10} state, it can be seen that the electron densities are localized on the phenol and new formed H-H_1. The electron densities of H-H_1 increase considerably when being excited to the LUMO, which implies that the newly formed H-H_1 bond is strengthened. In the P-S_{10} state, the electron densities are transferred from phenol moiety to BTMA moiety and those of H-H_1 hardly changed. The energy gap between HOMO and LUMO reflects the biological activity, optical

polarizability and chemical hardness-softness of the molecule. A small frontier orbital gap is generally associated with a high-chemical reactivity and low kinetic stability [57]. The transition energy of RC-S_1 is calculated to be 0.154 au, which is larger than that of TS-S_{10} and smaller than that of P-S_{10}. It can be seen that TS-S_{10} has higher chemical reactivity than RC-S_1 and P-S_{10}.

3.6 Dehydrogenation Mechanism Analysis

Figure 6 shows the dehydrogenation mechanism of phenol-BTMA through intermolecular dihydrogen bond in the excited S_1 state. The electronegativity of oxygen atom is larger than that of hydrogen atom, while the electronegativity of boron atom is smaller than that of hydrogen bond. Therefore, the H atom of O-H bond has positive charge and the H atoms of B-H bond have negative charge. In Figure 6-1, two intermolecular dihydrogen bonds are formed between phenol and BTMA molecules in the ground state. It has been demonstrated previously that no dehydrogenation reaction occurs in the ground state of dihydrogen bonded phenol-BTMA. When excited to the S_1 state, the O-H bond is cleaved and the dihydrogen bond interaction O-H•••H_1-B is considerably strengthened. The transition state theory (TST) method is performed here in order to study the dehydrogenation reaction of phenol-BTMA. Based on the geometric structure of phenol-BTMA in the S_1 state, TS-S_{10} and TS-S_{11} are found in order to study the dehydrogenation mechanism of phenol-BTMA. In Figure 6-2A, an intermediate product hydrogen molecule is formed, and the only imaginary frequency denoted at -337.12 cm^{-1} points to the direction of B atom but not the formation of hydrogen molecule. In Figure 6-2B, the hydrogen atom of O-H bond

transferred to the B-H bond of BTMA and a transitional product H•••H_1 is formed. After losing the hydrogen atom of B-H_1 bond, the molecular weight of $(CH_3)_3N$-BH_2^+ is consistent with the mass spectroscopic (71) in reference 39. The only imaginary frequency of TS-S_{10} is denoted at -745.46 cm^{-1} and points to the direction of the formation of hydrogen molecule. Moving away from BTMA molecule, the newly formed O•••H-H_1 is effected by the O atom through intermolecular dihydrogen bond interaction. In the P-S_{10} state, the dehydrogenation process is completed and the newly formed hydrogen molecule breaks away from the interaction of O atom. Figure 6 gives a simple theoretical model which describes the dehydrogenation process of phenol-BTMA in the excited S_1 state.

4. Conclusion

The dehydrogenation process of phenol-BTMA is discussed in this work. Time dependenst density functional theory (TDDFT) is performed here for studying the excited state of phenol-BTMA, and transition state theory (TST) is used to find the transitional product of dehydrogenation reaction. The analysis of geometric structures and infrared spectra of phenol-BTMA indicates that dehydrogenation processes does not occur in the ground state, which is also demonstrated by the potential energy curves in the ground state. When excited to the S_1 state, dihdyrogen bond O-H•••H_1-B is considerably strengthened and B-H_1 is cleaved simultaneously. A transition state is found when scanning the potential energy curve of phenol-BTMA in the S_1 state. The only imaginary frequency located at -745.46 cm^{-1} towards the formation of H-H_1, which confirms the existence of transition state. A transitional product O•••H-H_1 is

formed in the transition state. In the product complex state, the dehydrogenation process is completed and a hydrogen molecule is formed. This work provides a theoretical model for the dehydrogenation reaction of phenol-BTMA in the excited S_1 state, and will provide insight into the study of some proton-transferring chemical reaction.

Acknowledgments

This work is supported by National Natural Science Foundation of China (Grant No. 11274096), Innovation Scientists and Technicians Troop Construction Projects of Henan Province (Grant No.124200510013) and Supported by Program for Innovative Research Team (in Science and Technology) in University of Henan Province (Grant No. 13IRTSTHN016).

References

1. E. Pines, D. Pines, Y. -Z. Ma and G. R. Fleming, *ChemPhysChem.*, 2004, **5**, 1315-1327.
2. T. K. Ghanty, V. N. Staroverov, P. R. Koren and E. R. Davidson, *J. Am. Chem. Soc.*, 2000, **122**, 1210-1214.
3. C. E. H. Dessent and K. Müller-Dethlefs, *Chem. Rev.*, 2000, **100**, 3999-4022.
4. F. Yu, P. Li, G. Li, G. Zhao, T. Chu and K. Han, *J. Am. Chem. Soc.*, 2011, **133**, 11030-11033.
5. H. Otaki and K. Ando, *Phys. Chem. Chem. Phys.*, 2011, **13**, 10719-10728.
6. J.-S. Chen, P.-W. Zhou, G.-Y. Li, T.-S. Chu and G.-Z. He, *J. Phys. Chem. B*, 2013, **117**, 5212-5221.
7. G.-J. Zhao and K.-L. Han, *Biophys. J.*, 2008, **94**, 38-46.
8. I. Alkorta, I. Soteras, J. Elgueroa and J. E. Del Bene, *Phys. Chem. Chem. Phys.*, 2011, **13**, 14026-14032.
9. K. -L. Han, G. -J. Zhao, Hydrogen Bonding and Transfer in the Excited State; Wiley: WILEY-BLACKWELL, John Wiley & Sons Ltd, Chichester PO19 8SQ, UK, 2010; Volume I & II, Chapter 6, pp 149-158.
10. G. -J. Zhao and K. -L. Han, *Acc. Chem. Res.*, 2012, **45**, 404-413.
11. Y. F. Liu, Y. G. Yang, K. Jiang, D. H. Shi and J. F. Sun, *Phys. Chem. Chem. Phys.*, 2011, **13**, 15299-15304.
12. Y. F. Liu, D. P. Yang, D. H. Shi and J. F. Sun, *J. Comput. Chem.*, 2011, **32**, 3475-3484.

13. Y. F. Liu, J. X. Ding, R. Q. Liu, D. H. Shi and J. F. Sun, *J. Comput. Chem.*, 2009, **30**, 2723-2727.

14. Y. F. Liu, J. X. Ding, D. H. Shi and J. F. Sun, *J. Phys. Chem. A*, 2008, **112**, 6244-6288.

15. G. -J. Zhao and K. -L. Han, *J. Phys. Chem. A*, 2007, **111**, 2469-2474.

16. G. -J. Zhao, J. -Y. Liu, L. -C. Zhou and K. -L. Han, *J. Phys. Chem. B*, 2007, **111**, 8940-8945.

17. G. J. Zhao, B. H. Northrop, K. -L. Han and P. J. Stang, *J. Phys. Chem. A*, 2010, **114**, 9007-9013.

18. H. Jacobsen, *Chem. Phys.*, 2008, **345**, 95-102.

19. S. J. Grabowski, W. A. Sokalski and J. Leszczynski, *J. Phys. Chem. A*, 2005, **109**, 4331-4341.

20. P. C. Singh, D. K. Maity and G. N. Patwari, *J. Phys. Chem. A*, 2008, **112**, 5930-5934.

21. S. Trudel and D. F. R. Gilson, *Inorg. Chem.*, 2003, **42**, 2814-2816.

22. I. Alkorta, F. Blanco and J. Elguero, *J. Phys. Chem. A*, 2010, **114**, 8457-8462.

23. N. -N Wei, C. Hao, Z. Xiu and J. Qiu, *Phys. Chem. Chem. Phys.*, 2010, **12**, 9445-9451.

24. H. Jacobsen, *Phys. Chem. Chem. Phys.*, 2009, **11**, 7231-7240.

25. R. Custelcean and J. E. Jackson, *Chem. Rev.*, 2001, **101**, 1963-1980.

26. W. T. Klooster, T. F. Koetzle, P. E. M. Siegbahn, T. B. Richardson and R. H. Crabtree, *J. Am. Chem. Soc.*, 1999, **121**, 6337-6343.

27. M. A. Esteruelas, A. M. López, M. Mora and E. Oñate, *ACS. Catal.*, 2015, **5**, 187-191.

28. S. A. Kulkarni, *J. Phys. Chem. A*, 1999, **103**, 9330-9335.

29. Q. Liu and R. Hoffmann, *J. Am. Chem. Soc.*, 1995, **117**, 10108-10112.

30. I. Rozas, I. Alkorta and J. Elguero, *Chem. Phys. Lett.*, 1997, **275**, 423-428.

31. O. A. Filippov, N. V. Belkova, L. M. Epstein and E. S. Shubina, *J. Organomet. Chem.*, 2013, **747**, 30-42.

32. G. N. Patwari, *J. Phys. Chem. A*, 2005, **109**, 2035-2038.

33. P. C. Singh and G. N. Patwari, *Chem. Phys. Lett.*, 2006, **419**, 5-9.

34. G. N. Patwari, T. Ebata and N. Mikami, *J. Chem. Phys.*, 2001, **114**, 8877-8879.

35. P. C. Singh and G. N. Patwari, *Chem. Phys. Lett.*, 2006, **419**, 265-268.

36. P. C. Singh and G.N. Patwari, *J. Phys. Chem. A*, 2007, **111**, 3178-3183.

37. G. N. Patwari, T. Ebata and N. Mikami, *Chem. Phys.*, 2002, **283**, 193-207.

38. G. N. Patwari, T. Ebata and N. Mikami, *J. Chem. Phys.*, 2000, **113**, 9885-9888.

39. G. N. Patwari, T. Ebata and N. Mikami, *J. Phys. Chem. A*, 2001, **105**, 10753-10578.

40. P. C. Singh, D. K. Maity and G. N. Patwari, *J. Phys. Chem. A*, 2008, **112**, 5930-5934.

41. G. -J. Zhao and K. -L. Han, *J. Chem. Phys.*, 2007, **127**, 0243061-0243066.

42. P. Jaramillo, K. Coutinho and S. Canuto, *J. Phys. Chem. A*, 2009, **113**, 12485-12495.

43. K. Sakota, C. Jouvet, C. Dedonder, M. Fujii and H. Sekiya, *J. Phys. Chem. A*, 2010, **114**, 11161-11166.

44. H. Zaher, A. E. Ashley, M. Irwin, A. L. Thompson, M. J. Gutmann, T. Krämera and D. ÓHare, *Chem. Commun.*, 2013, **49**, 9755-9757.

45. A. Fujii, G. N. Patwari, T. Bbata and N. Mikami, *Int. J. Mass. Spectrom.*, 2002, **220**, 289-312.

46. J M. Abboud, B. Németh, J. Guillemin, P. Burk, A. Adamson and E. R. Nerut, *Chem. Eur. J.*, 2012, **18**, 3981-3991.

47. Y. F. Liu, Y. G. Yang, K. Jiang, D. H. Shi and J. F. Sun, *Bull. Chem. Soc. Jpn.*, 2011, **84**, 191-195.

48. B. C. Garrett, D. G. Truhlar, R. S. Grev and A. W. Magnuson, *J. Phys. Chem.*, 1980, **84**, 1730-1748.

49. A. D. Isaacson and D. G. Truhlar, *J. Chem. Phys.*, 1982, **76**, 1380-1391.

50. V. L. Schramm, *J. Biol. Chem.*, 2007, **282**, 28297-28300.

51. V. L. Schramm, *Annu. Rev. Biochem.*, 1998, **67**, 693-720.

52. K. Laidler and C.King, *J. Phys. Chem.*, 1983, **87**, 2657-2664.

53. M. J. Frisch, G. W. Trucks, H. B. Schlegel, G. E. Scuseria, M. A. Robb, J. R. Cheeseman, G. Scalmani, V. Barone, B. Mennucci, G. A. Petersson, H. Nakatsuji, M. Caricato, X. Li, H. P. Hratchian, A. F. Izmaylov, J. Bloino, G. Zheng, J. L. Sonnenberg, M. Hada, M. Ehara, K. Toyota, R. Fukuda, J. Hasegawa, M. Ishida, T. Nakajima, Y. Honda, O. Kitao, H. Nakai, T. Vreven, J. A. Montgomery, Jr., J. E. Peralta, F. Ogliaro, M. Bearpark, J. J. Heyd, E. Brothers, K. N. Kudin, V. N.

Staroverov, T. Keith, R. Kobayashi, J. Normand, K. Raghavachari, A. Rendell, J. C. Burant, S. S. Iyengar, J. Tomasi, M. Cossi, N. Rega, J. M. Millam, M. Klene, J. E. Knox, J. B. Cross, V. Bakken, C. Adamo, J. Jaramillo, R. Gomperts, R. E. Stratmann, O. Yazyev, A. J. Austin, R. Cammi, C. Pomelli, J. W. Ochterski, R. L. Martin, K. Morokuma, V. G. Zakrzewski, G. A. Voth, P. Salvador, J. J. Dannenberg, S. Dapprich, A. D. Daniels, O. Farkas, J. B. Foresman, J. V. Ortiz, J. Cioslowski, and D. J. Fox, Gaussian, Inc., Wallingford CT, 2010.

54. A. D. Becke, *J. Chem. Phys.*, 1993, **98**, 5648-5652.

55. C. Lee, W. Yang and R.G. Parr, *Phys. Rev. B*, 1988, **37**, 785-789.

56. V. Lemaur, M. Steel, D. Beljonne, J. -L. Brédas and J. Comil, *J. Am. Chem. Soc.*, 2005, **127**, 6077-6086.

57. S. Luber, K. Adamczyk, E. T. J. Nibbering and V. S. Batista, *J. Phys.Chem. A*, 2013, **117**, 5269-5279.

Figure Captions:

Figure 1. The calculated bond lengths and angles of RC-S_0, RC-S_1, TS-S_{10}, P-S_{10}, TS-S_{11} and P-S_{11}.

Figure 2. The potential curves of RC in the ground state and the energy profile of RC-S_0, RC-S_1, TS and P.

Figure 3. The energy profiles of RC-S_0, RC-S_1, TS-S_{10}, P-S_{10}, TS-S_{11} and P-S_{11}.

Figure 4. The calcualted infrared spectra of the functional groups of RC-S_0, RC-S_1, TS-S_{10} and P-S_{10}, and their corresponding geometric structures.

Figure 5. The frontier molecular orbitals corresponding to the excited S_1 state and transition energy of RC-S_1, TS-S_{10} and P-S_{10}.

Figure 6. The dehydrogenation mechanism of phenol-BTMA in the excited S_1 state.

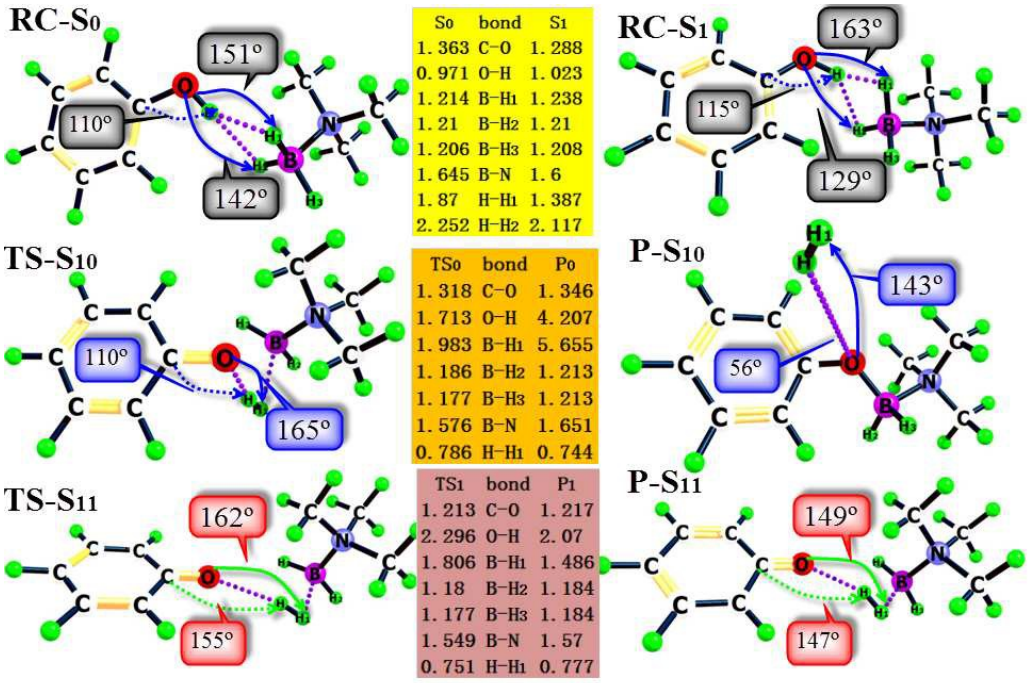

Figure 1

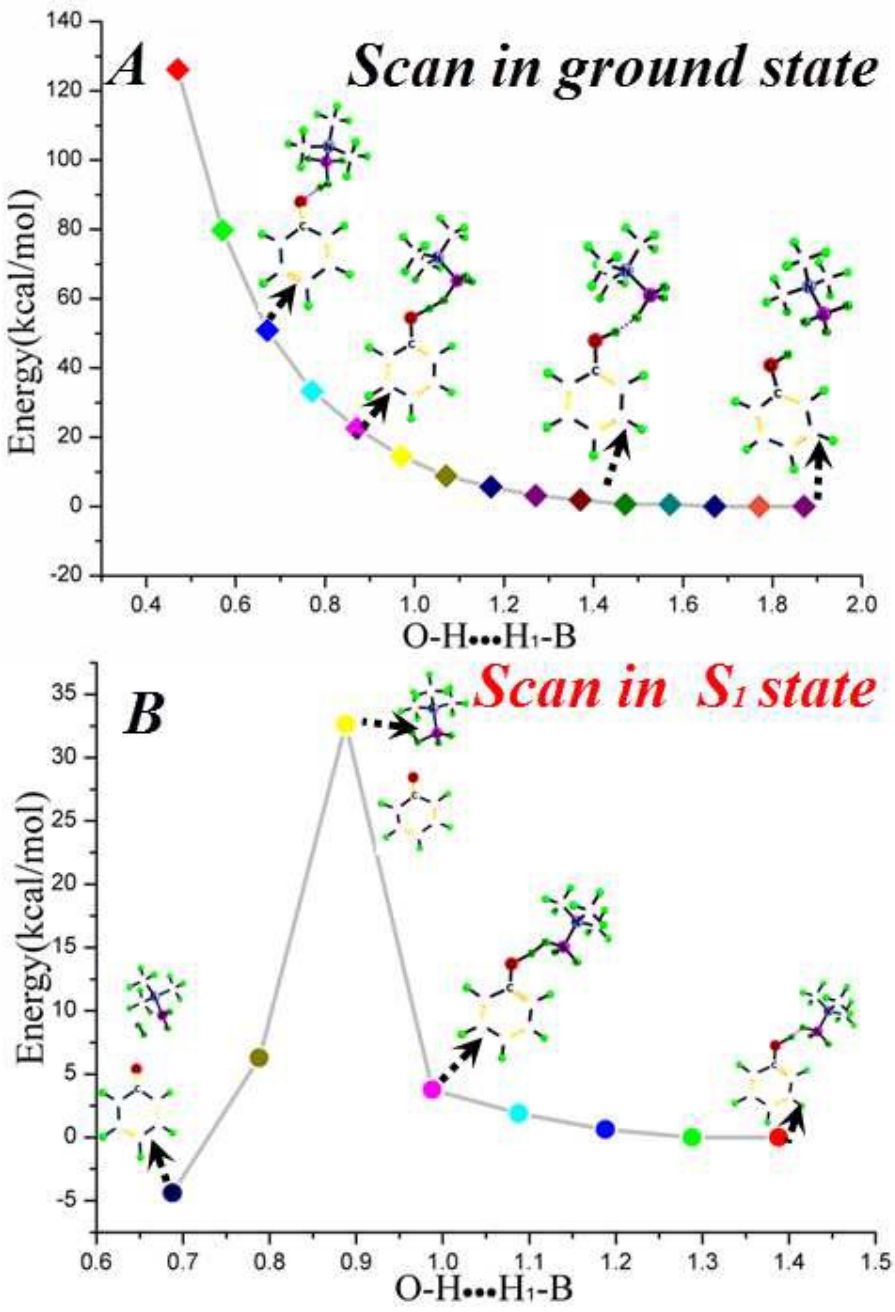

Figure 2

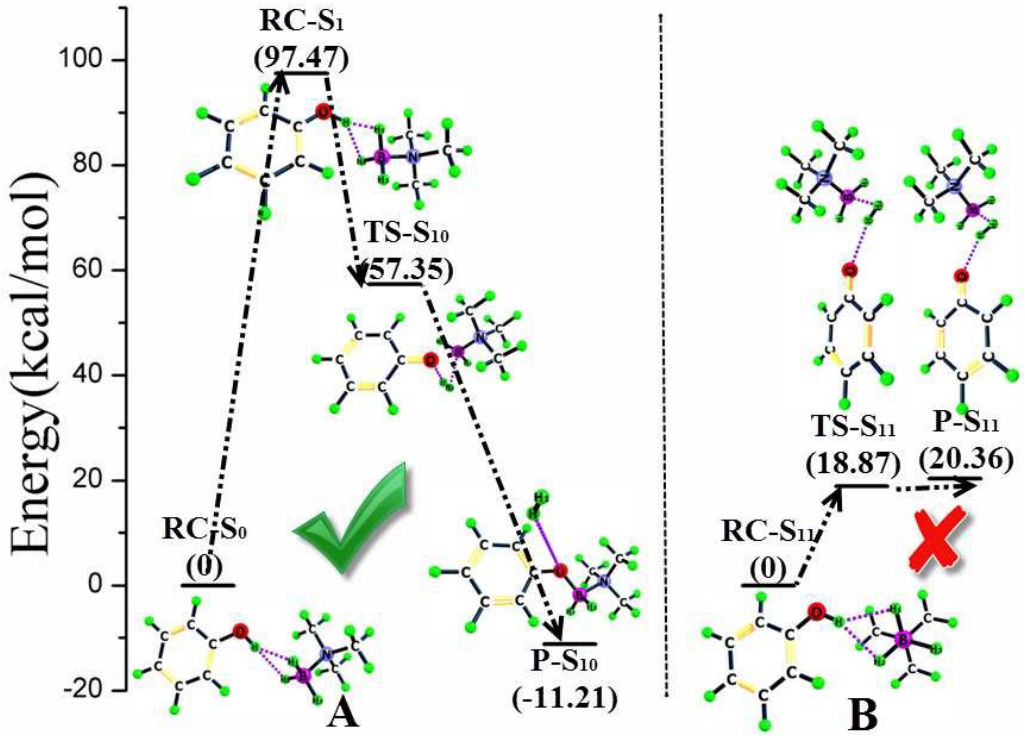

Figure 3

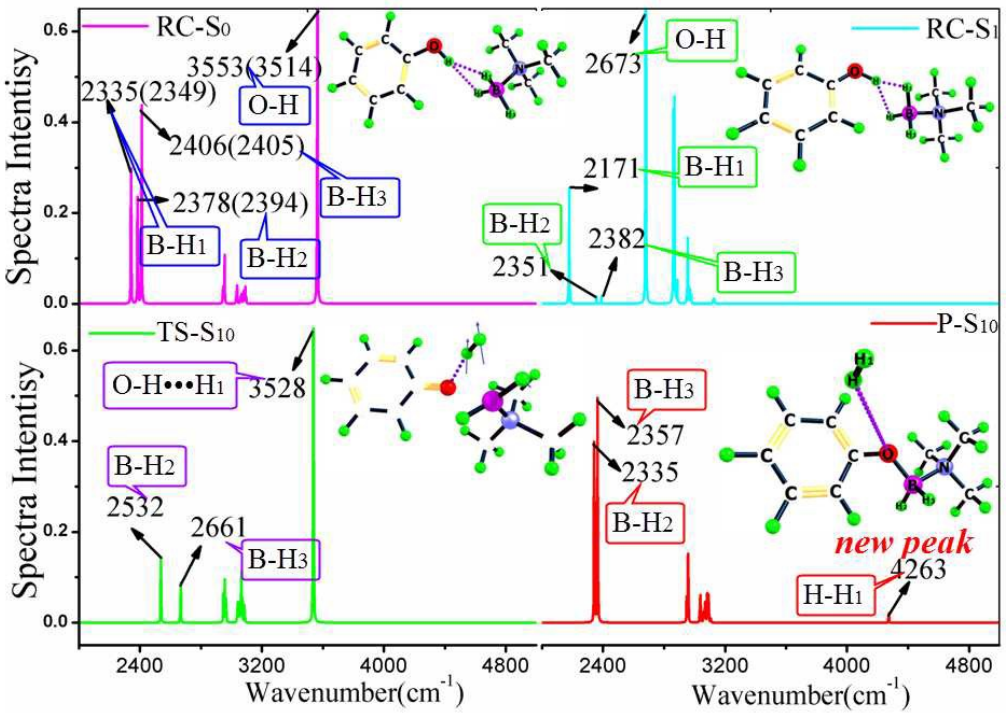

Figure 4

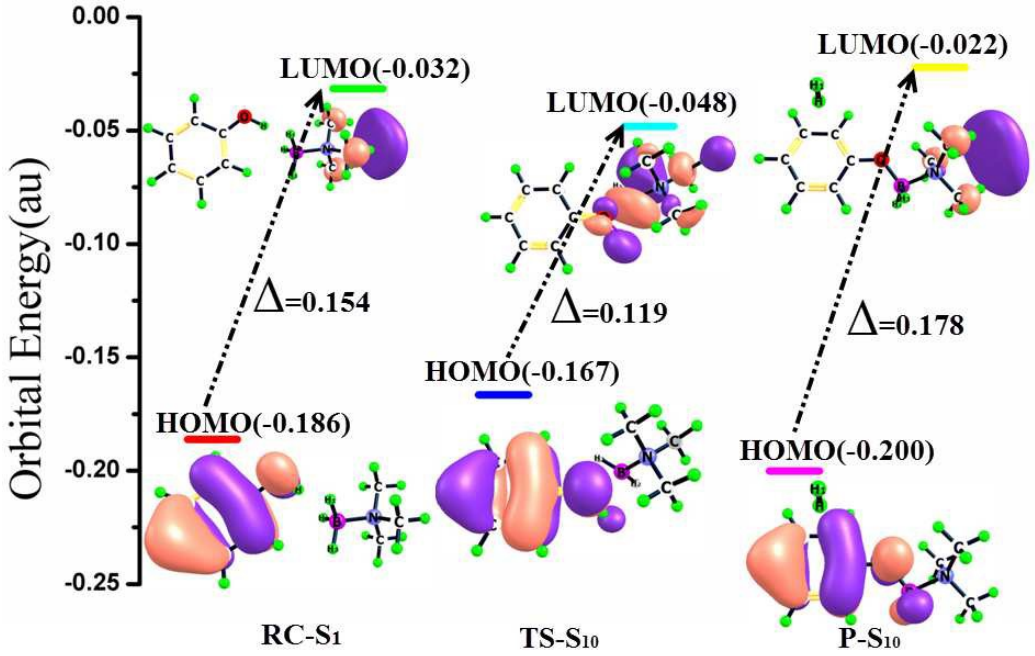

Figure 5

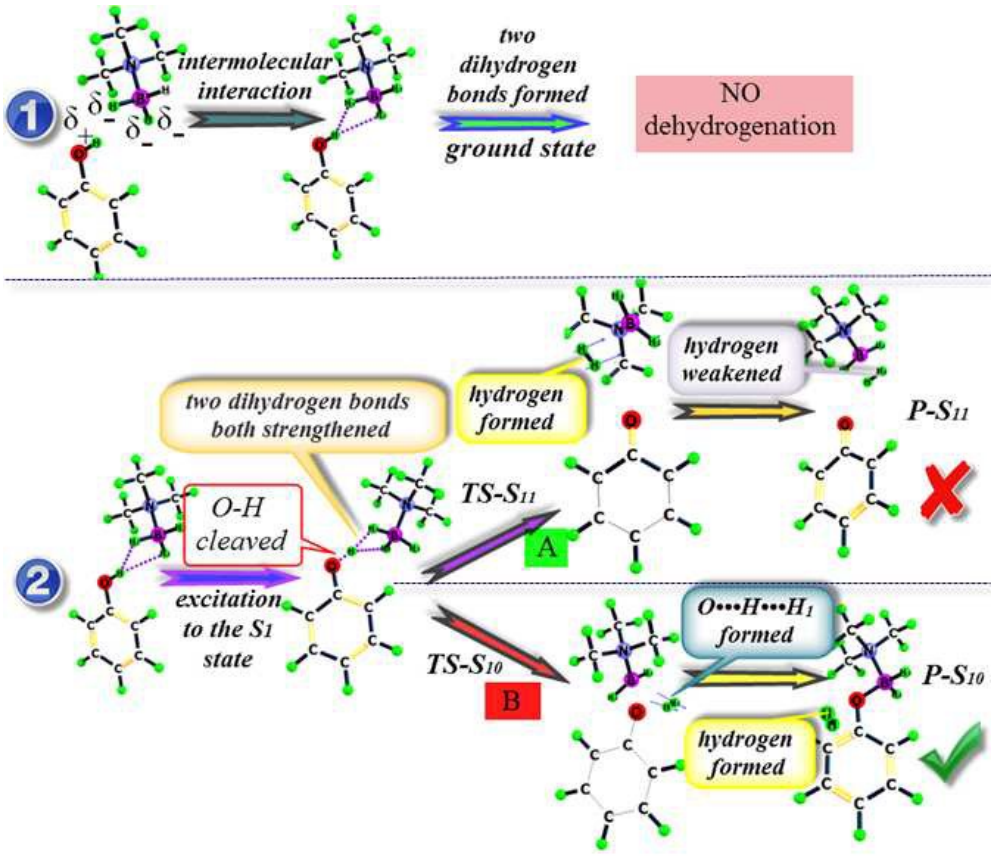

Figure 6